^{57}Fe Mossbauer study of metastable 304 stainless steel film with BCC structure

1995 J. Phys.: Condens. Matter 7 1921

(http://iopscience.iop.org/0953-8984/7/9/016)

J. Phys.: Condens. Matter 7 (1995) 1921–1931. Printed in the UK

^{57}Fe Mössbauer study of metastable 304 stainless steel film with BCC structure

Fa-Shen Li†, Ji-Jun Sun†§ and C L Chien‡

† Department of Physics, Lanzhou University, Lanzhou 730000, People's Republic of China
‡ Department of Physics and Astronomy, The John Hopkins University, Baltimore, Maryland 21218, USA

Received 18 August 1994, in final form 11 January 1995

Abstract. The metastable 304 stainless steel film with BCC structure, fabricated by using a vapour quenching method, is strongly ferromagnetic. The effect of the local environment on the hyperfine parameters, and the influence of the heat treatment and pressure on stability in the metastable phase, were studied by means of conventional and high-pressure ^{57}Fe Mössbauer spectroscopy. Each non-iron nearest-neighbour atom (Cr, Ni and Mn) of Fe atoms decreases the hyperfine field by an average of about 2.3 T and the isomer shift by about 0.01 mm s^{-1}. Moreover, each non-iron next-nearest-neighbour atom is estimated to reduce the hyperfine field by an average of about 1.2 T. It is found that the transformation from the metastable BCC state to the FCC state begins near 500 °C and is completed near 800 °C. No FCC phase appears under a pressure smaller than 36 kbar. In both cases, however, the magnetization direction of the sample is observed to reorientate, and shows a stronger tendency to the out-of-plane after annealing and under pressures up to 8 kbar, while it is closer to the in-plane under pressures larger than 8 kbar.

1. Introduction

The structure dependence of the magnetic properties of Fe-based alloys is one of the most interesting aspects of magnetism [1]. Ordinary BCC (body-centred cubic) α-Fe is strongly ferromagnetic, whereas FCC (face-centred cubic) γ-Fe is not. An interesting case in point is 304 stainless steel (SS). Ordinary 304 SS, with a nominal composition of 72 w.% Fe, 18 w.% Cr, 8 w.% Ni and 2 w.% Mn, normally appears in the FCC phase, which is non-magnetic. However, a metastable BCC 304 SS film is strongly ferromagnetic, and may be obtained by using a vapour quenching method [2].

An investigation of the magnetic properties of the metastable BCC phase has been reported recently [3, 4]. The BCC phase was found to have a spontaneous magnetization of 130 emu g^{-1}, while the magnetization of the 304 SS target material was about 1 emu g^{-1} under an external field of 14 kOe. Thus, the strong structure dependence of the magnetic properties is vividly demonstrated in BCC and FCC 304 SS. It was also shown that the magnetic easy axis is in the plane of the BCC 304 SS film, and the anisotropy field was estimated to be 19 kG. The BCC 304 SS film is magnetically soft, with a coercivity of about 50 Oe, and the Curie temperature was found to be greater than 550 °C.

As a metastable BCC phase, which is rather different from those metastable amorphous alloys, it is very helpful to study the influence of the local environment on the magnetic

§ Present address: National Laboratory for Superconductivity, Institute of Physics, Chinese Academy of Sciences, PO Box 603-35, Beijing 100080, People's Republic of China.

0953-8984/95/091921+11$19.50

properties in order to obtain further understanding about the metastable state. Furthermore, for a metastable phase, its stability is rather important because of its possible technological application. Just like amorphous alloys, quantities such as pressure, temperature and so on have an influence on the physical properties of amorphous alloys. In addition, it is expected that the metastable BCC phase should be easier to transform from the BCC state to the FCC state under pressure than α-Fe. It is well known that Mössbauer spectroscopy, including spectroscopy at various extreme conditions, such as under high pressure and high magnetic field, has advantages in the investigation of the local properties and phase structure of magnetic materials. Therefore, in this work, the metastable BCC 304 SS film was systematically studied by means of ^{57}Fe Mössbauer spectroscopy, with the emphasis put on the effect of the local environment on the magnetic properties, and the stability of the metastable phase under the conditions of heat treatment and pressure.

2. Experiment

Thin films of 304 SS were obtained using a high-rate DC magnetron sputtering system with a FCC 304 SS target. Films of a few μm in thickness were deposited on mica and Al_2O_3. However, x-ray diffraction shows the as-sputtering 304 SS is single-phase BCC, with no evidence of either the FCC or amorphous phase. The sputtering films were annealed under temperature from 450 °C to 800 °C for 20 min.

^{57}Fe Mössbauer spectra were taken at room temperature with a standard set-up equipped with ^{57}Co(Rh). The high-pressure cell was a Chester-Jones-type high-pressure set-up with specially designed B_4C anvils as described elsewhere [5]. The pressure was calibrated by the pressure dependence of isomer shift (IS) of a β-Sn foil mounted together with the sample [6]. The IS at ^{57}Fe nuclei is relative to α-Fe at room temperature.

3. Results and discussion

3.1. The analysis of the Mössbauer spectra

Figure 1 shows the Mössbauer spectrum of the as-sputtering metastable 304 SS film. It can be seen that the Mössbauer spectrum of the as-sputtered 304 SS film exhibits a magnetic splitting spectrum. This fact indicates further that the 304 SS film is in a magnetic BCC state, which is consistent with findings from x-ray diffraction (with lattice parameter $a = 2.87$ Å). However, it can be seen clearly that the magnetic splitting Mössbauer spectrum consisted of six broadening lines, which is similar to that of amorphous Fe-based alloys. However, the broadening sextet cannot be due to the amorphous state, since there is no evidence of the amorphous phase in x-ray diffraction. The broadening is attributed to the difference in the environment of the Fe atom in the 304 SS film; the spectrum is actually a superposition of several sextets, each with different Mössbauer hyperfine interaction parameters, depending on the number of iron neighbours of the resonantly absorbing ^{57}Fe atom.

According to the analysis of ordered Fe–Al alloys by Czjzek and Berger [7], the details of the hyperfine spectra of these alloys can be described at least approximately if one assumes that individual Al atoms in the neighbourhood of an iron atom independently affect fields at the nucleus of the iron atom. The effect of Al neighbours decreases with increasing distance from a given iron atom. Over regions of limited concentration, the effect per Al atom in a given coordination shell is approximately constant. In other words, the hyperfine field of Fe atoms depends strongly on the number and distance of Fe neighbour atoms. For BCC

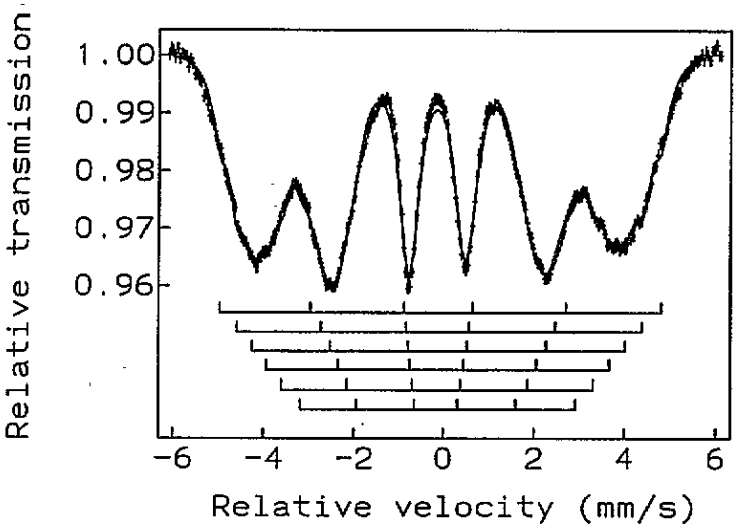

Figure 1. Mössbauer spectrum at room temperature for the as-sputtering 304 SS film.

structure, each atom has eight nearest-neighbour sites. So, for the BCC 304 SS, each iron atom has nine types of nearest-neighbour configuration, i.e. $(m, 8-m)$, with $m = 1$–8; the numbers in the brackets refer to the number of nearest neighbours of iron and non-iron (Cr, Ni and Mn) atoms, respectively. According to the binomial distribution

$$P_m = C_8^m x^m (1-x)^{8-m} \tag{1}$$

where x is the concentration of Fe atoms (with $x = 71.3$ at.%) and m is the number of nearest-neighbour Fe atoms. However, only the most probable configurations ($P_m > 1\%$) were taken into account, which sum up to an overall probability of greater than 99%. So only six subspectra, corresponding to the six most probable configurations, i.e. $m = 8$–3, were used to fit the Mössbauer spectrum of the BCC 304 SS film. Their relative contributions were, however, taken as free parameters in the computer-fit procedure to allow for possible inhomogeneities of the atomic distribution. The corresponding subspectra are also shown in figure 1.

In addition, Hesse's method, which can give information about the distribution of the hyperfine field [8], was also used to fit the as-sputtering 304 SS for comparison with the method mentioned above. The distribution of the hyperfine field of the as-sputtering 304 SS film is shown in figure 2.

3.2. The influence of the local environment

Figure 3 shows the hyperfine parameters as a function of the number of nearest-neighbour Fe atoms. It is clear from figure 3(*a*) that the hyperfine field increases linearly with the number of nearest-neighbour iron atoms, which is consistent with that for Fe–Al alloys [7]. Each non-iron nearest-neighbour atom of the Fe atoms decreases the hyperfine field of ^{57}Fe on average by about $\Delta H_1 = 2.3$ T, which is slightly smaller than the 3.2 T for Fe–Cr alloys [9]. The smaller decrease can be attributed to the magnetic atoms Ni, Mn in non-iron atoms for the BCC 304 SS film. However, the hyperfine field with eight Fe nearest-neighbours is only 31.0 T, which is lower by 2 T than that of α-Fe (33.1 T). This may be due to the influence of non-iron next-nearest-neighbour atoms.

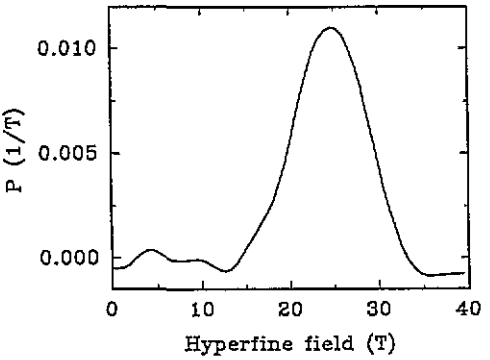

Figure 2. The distribution of the hyperfine field of the as-sputtering 304 SS film.

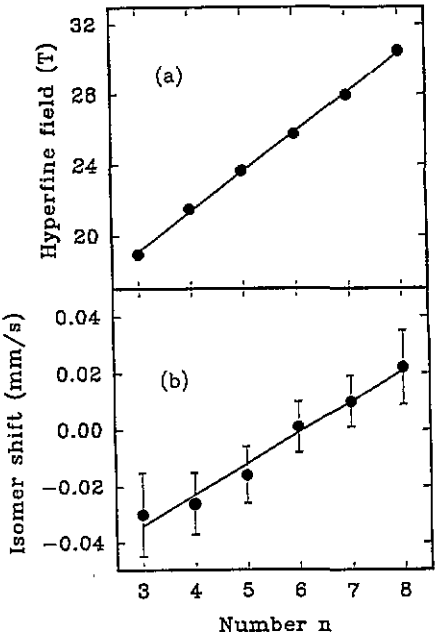

Figure 3. The Mössbauer parameters of the as-sputtering 304 SS film as a function of the number of the nearest-neighbour Fe atoms; *(a)* hyperfine field, *(b)* isomer shift.

For BCC structure, each atom has six next-nearest-neighbour sites. According to the analysis mentioned above, it is reasonable to assume that each non-iron atom decreases the same hyperfine field, ΔH_2. So considering the contribution of the next-nearest neighbours, the hyperfine field with eight nearest-neighbour Fe atoms, $H(8)$, can be written as

$$H(8) = H(8,6) - \sum_{n=0}^{6}(6-n)P(n,6-n)\Delta H_2 \tag{2}$$

where the $H(8,6)$ is the hyperfine field with eight nearest-neighbour and six next-nearest-neighbour configurations, n is the number of next-nearest-neighbour Fe atoms, and $P(n,6-n)$ is the possibility of the binomial distribution with the n next-nearest neighbour Fe atoms. As a simple estimate, using the result of Fe–Cr [9], $H(8,6) = 33.5\,\mathrm{T}$, so it may be obtained that ΔH_2 is about equal to 1.2 T, which is smaller than $\Delta H_2 = 2.2\,\mathrm{T}$ in Fe–Cr alloys. However, $\Delta H_1 > \Delta H_2$, which clearly indicates that the effect of the non-iron atoms decreases with increasing distance from a given iron atom.

For the IS shown in figure 3(*b*), it is clear that the isomer shift increases linearly with the number of nearest-neighbour Fe atoms, i.e. the non-iron atoms cause the decrease of the isomer shift. This is similar to the behaviour of Fe–Cr and Fe–V alloys [9, 10]. Each non-iron atom decreases the isomer shift by $\Delta \mathrm{IS}_1 = 0.01\,\mathrm{mm\,s^{-1}}$. This means that the appearance of the non-iron atoms in the vicinity of the probe atom increases the effective charge density of the s-like electron at the site of Fe. This is contrary to the behaviour of Fe–Al and Fe–Si alloys [11, 12], where the effective charge density of s-like electrons at the Fe nucleus is diminished by neighbouring Al or Si atoms. The difference between the BCC 304 SS, Fe–Cr or Fe–V, and Fe–Al or Fe–Si alloys may be mainly due to the different magnitude of the

contribution of the electronegativity and the electron density at the Wigner–Seitz atomic-cell boundaries of non-iron atoms according to the Miedema and van der Woude model [13]. The former mainly results from the relative larger electronegativity difference between Fe and Cr or V, which increases the density of the s-like electrons; the latter is due to the relative larger difference in electron density at the Wigner–Seitz atomic-cell boundaries between the Fe and Al or Si, which causes s→d-electron conversion and decreases the density of the s-like electrons [14].

In fact, ΔH_1 and ΔIS_1 provide information on local changes in the spin density and the charge density at ^{57}Fe nuclei. For non-iron atoms as nearest neighbours of the Fe atom in a 304 SS film, the hyperfine field is reduced, which means that the effective density of spin-down electrons is diminished and the charge density is increased. Therefore, the decrease of the hyperfine field must be realized by an increase of spin-up electron density [10]. For the nearest-neighbour atoms, the ratio $\Delta H_1/\Delta IS_1$ is $205\,T\,mm^{-1}\,s^{-1}$. From the relation between the changes of the isomer shift and the corresponding changes of the number of s-like electrons, $\delta IS/\delta N_s = 2.05\,mm\,s^{-1}$ [15], it can be easily calculated that the relationship between the hyperfine field and the corresponding number of polarized electrons N_s, is $\Delta H_1/\Delta N_s = 420\,T$. For ΔIS_1, using $\delta IS/\delta N_s = 2.05\,mm\,s^{-1}$, one can calculate that the effective increase of the charge density is equivalent to the increase of the number of s-like electrons, by 0.005 for one non-iron atom as the nearest neighbour in a BCC 304 SS film.

Figure 2 shows the distribution of the hyperfine field of the BCC as-sputtering 304 SS derived from the Hesse method. The full width at half maximum of the distribution of the hyperfine field is about 9.3 T. It can be seen that the maximum value of the distribution of the hyperfine field is at $H = 24.6\,T$, which is smaller than the 25.8 T of the most probable configuration with six iron nearest neighbours. The average hyperfine field 24.3 T is in good agreement with that obtained by six subspectra (24.9 T). Assuming that the average moment of the iron atom is proportional to the average hyperfine field with hyperfine coupling constant $15.0\,T\,\mu_B^{-1}$ deduced from pure α-Fe, where the magnetic moment, the magnetization and the hyperfine field are $2.2\mu_B$, $220\,emu\,g^{-1}$ and 33.1 T, respectively, the magnetic moment of the iron atom in BCC 304 SS can be derived to be about $1.7\,\mu_B$. Since the 304 SS has 72% of Fe, this accounts very well for the observed magnetization of $130\,emu\,g^{-1}$ [3]. Therefore, it can be concluded that in the BCC 304 SS, only the Fe atoms contribute significantly to the magnetization.

3.3. The influence of the heat treatment

Figure 4 shows the Mössbauer spectra of the 304 SS film after annealing at different temperatures. The Mössbauer spectrum of the BCC 304 SS annealed at 450 °C is nearly the same as that of the as-sputtering BCC 304 SS except for the relative intensity of the second and fifth peaks. In Mössbauer spectra, the relative intensity ratio between second(fifth) and first(sixth) peaks can be written as

$$\frac{A_{2,5}}{A_{1,6}} = \frac{4\sin^2\theta}{3(1+\cos^2\theta)} \qquad (3)$$

where θ is the angle between the γ-ray direction and the magnetic moment direction. For the as-sputtering BCC 304 SS, the ratio $A_{2,5}/A_{1,6}$ is 0.74, which deviates slightly from that of the random orientation of the magnetic moment. This fact shows that the average magnetic moment direction tends to be in the in-plane direction for the BCC 304 SS, which is consistent with findings from magnetic measurements [4]. For the annealed sample, the ratio $A_{2,5}/A_{1,6}$

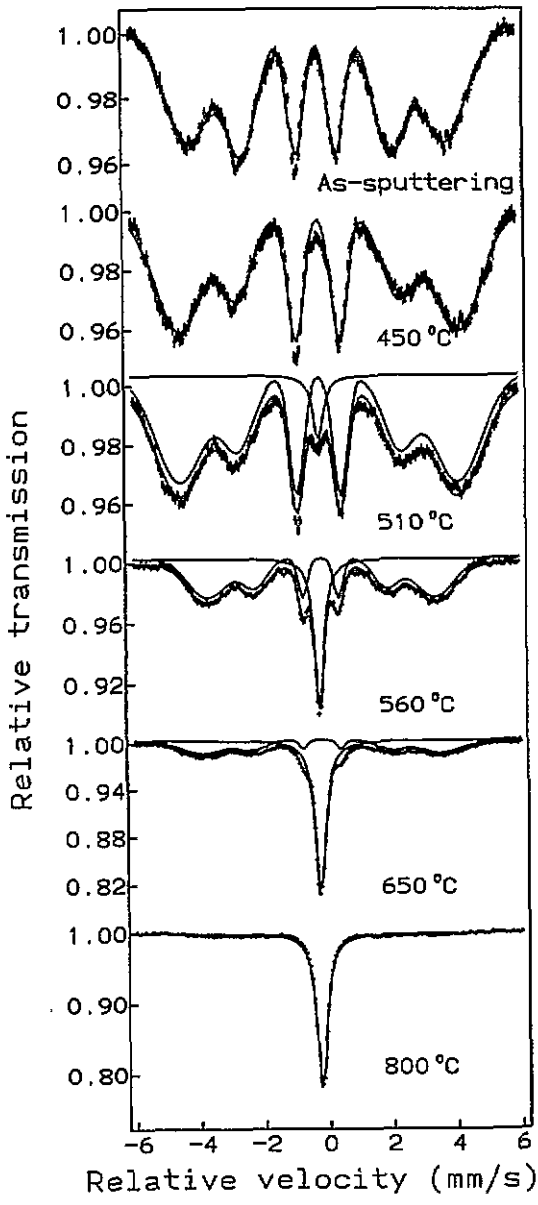

Figure 4. Mössbauer spectra at room temperature for the BCC 304 SS film at different annealing temperature.

is decreased to 0.46, hence a rotation of the average magnetic moment direction to the out-of-plane has taken place. This out-of-plane anisotropy was also found in the amorphous alloy under certain temperature annealing [16]. For the BCC α-Fe, the easy magnetization axis is [100]. The easy magnetization direction of the as-sputtering BCC 304 SS is dominated by the geometrical demagnetization effect, the stress and the possible directional growth of the sputtering film, which can all lead to form the magnetic texture. The high-temperature annealing serves as the stress-release process, so the easy axis direction shows a stronger tendency to the out-of-plane.

For the BCC 304 SS annealed at 510 °C, the single peak is observed in its Mössbauer spectrum, which indicates that the non-magnetic FCC state of 304 SS appears in the metastable

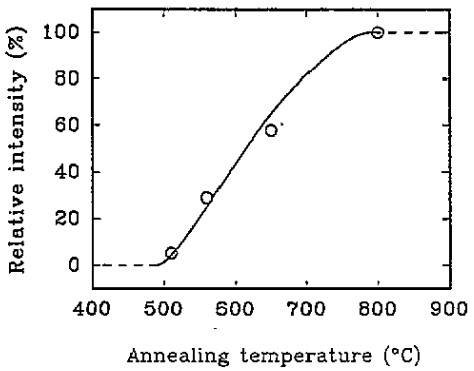

Figure 5. Annealing temperature dependence of the relative intensity of the FCC 304 SS film.

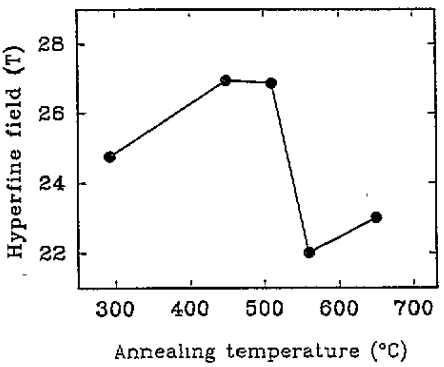

Figure 6. Annealing temperature dependence of the hyperfine field of the BCC 304 SS film.

BCC 304 SS. Moreover, the relative intensity of the FCC 304 SS from the Mössbauer spectrum is about 5.3%. Figure 5 shows the annealing temperature (T_A) dependence of the relative intensity of the FCC 304 SS. One can see that the transformation from the BCC to the FCC state begins near 500 °C, which is similar to that from x-ray diffraction [3]. In the annealing temperature range 500 °C $\leqslant T_A <$ 800 °C, the BCC and FCC states coexist in the annealed samples, the component of the FCC state increases with annealing temperature. Furthermore, the $A_{2,5}/A_{1,6}$ of BCC 304 SS in the annealed samples is the same, about 0.41 $\sim$ 0.44, and very close to that in the sample annealed at 450 °C. This demonstrates that the easy magnetization direction of the BCC 304 SS annealed at 450 °C $\leqslant T_A <$ 800 °C is nearly independent of the annealing temperature. In other words, the annealing temperature in the range 450 °C $\leqslant T_A <$ 800 °C has no influence on the magnitude of the rotation of the easy magnetization axis; the minimum value of θ due to the annealing is 43.3° rather than 57.7° corresponding to the as-sputtering 304 SS film.

For the sample annealed at 800 °C, the Mössbauer spectrum consists only of a single peak, which is clearly characteristic of the FCC state of 304 SS. This shows that the transformation is completed near 800 °C. The single peaks observed in all annealed samples are the same as that in the FCC 304 SS target material with the IS of about $-0.11\,\mathrm{mm\,s^{-1}}$ [3].

In the entire annealing temperature range, the average hyperfine field of the BCC state in the 304 SS sample changes a little, as is shown in figure 6. One can see that the hyperfine field increases by about 2.0 T after annealing at 450 °C and 510 °C, which may be attributed to the BCC structure being more regular after annealing at the lower temperature. The hyperfine field starts to reduce when the FCC state appears, which is 22.0 T after annealing at 560 °C. A similar result was also found for the spontaneous magnetization of the annealed BCC 304 SS measured at 30° by Childress and co-workers [3].

3.4. The influence of pressure

It is obvious that the packed density of FCC 304 SS is larger than that of BCC 304 SS. As expected, the metastable BCC state of 304 SS under pressure may be transformed to the FCC state. Therefore, high-pressure ^{57}Fe Mössbauer spectra of metastable BCC 304 SS were measured under a pressure up to 36 kbar. Figure 7 shows Mössbauer spectra of BCC 304 SS at different pressures. The pressure dependencies of hyperfine parameters are listed in figure 8. The hyperfine field and isomer shift of BCC 304 SS vary very slightly, where the decreasing maximum is 0.3 T for the hyperfine field and $0.02\,\mathrm{mm\,s^{-1}}$ for the IS, and

no non-magnetic single peak is observed, in the entire pressure range studied. This mainly results from the smaller pressure. This shows that the BCC 304 SS cannot transform to the FCC state and is stable under pressures up to 36 kbar. Furthermore, the changing tendency of the hyperfine parameters is similar to that in α-Fe [17]. In fact, the phase transformation from α-Fe to ε-Fe (HCP) was found to be at about 130 kbar at room temperature [18], while that from α-Fe to γ-Fe was under 110 kbar at about 800 °C or under lower pressure at higher temperature [19].

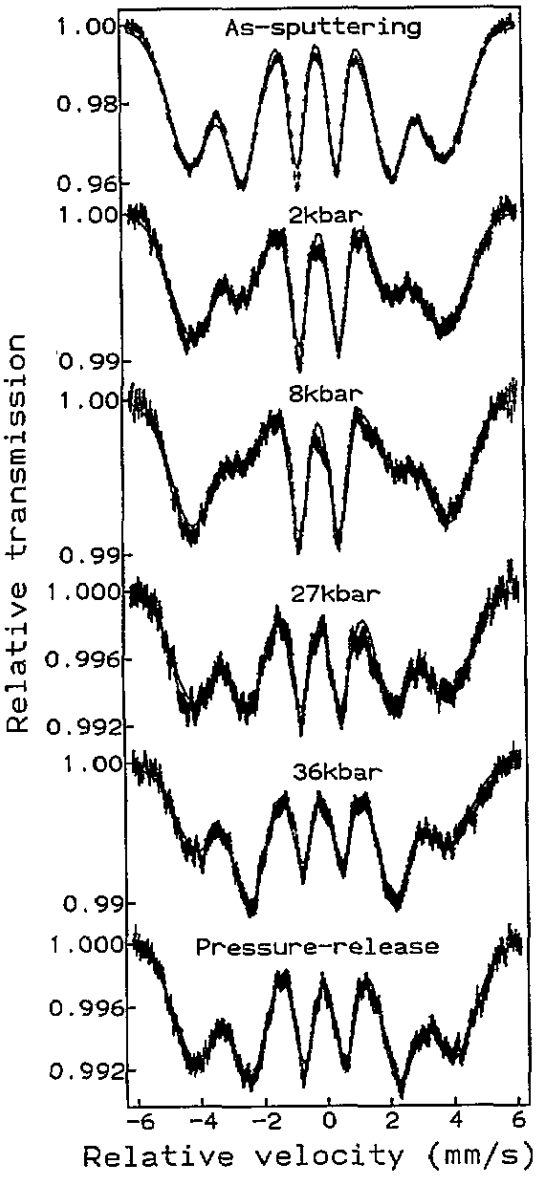

Figure 7. Mössbauer spectra at room temperature for the BCC 304 SS film at different pressures.

The interesting variation is still the relative intensity ratio $A_{2,5}/A_{1,6}$. From figure 7, it can be seen that the Mössbauer spectra of the BCC 304 SS under 2 kbar is similar to

that annealed at 450 °C, and $A_{2,5}/A_{1,6} = 0.44$. It is found that the value of $A_{2,5}/A_{1,6}$ monotonically decreases with increasing pressure up to 8 kbar. Figure 9 shows the pressure dependence of the angle θ between the γ-ray direction and the magnetic moment direction from (3). The average value of θ is about 40.0° at a pressure of 8 kbar rather than 57.7° for the as-sputtering 304 SS film. This means that the magnetic moment rotates to the out-of-plane at pressures up to 8 kbar, which is the same as that in the annealing BCC 304 SS. The pressure perpendicular to the sample plane may counteract to a certain extent the internal stress in the sputtering BCC 304 SS, and leads to the magnetic moment tend to the out-of plane, i.e. a more stable state. Furthermore, this also indicates that the original internal stress in the sample lies in the out-of-plane direction and is compression stress, which causes the expansion of the thin film and normally exists in metallic films with larger thicknesses [20]. At a pressure of 8 kbar, the magnitude of the rotation of the magnetic moment is slightly larger than that in the annealing treatment, which demonstrates that the pressure influences more directly the magnitude of the rotation of the magnetic moment to the out-of-plane than does the annealing. At the same time, it implies that the annealing cannot lead to total stress-release, while the pressure can counteract the stress to a greater extent. When the pressure is larger than 8 kbar, one can see that $A_{2,5}/A_{1,6}$ starts to increase with pressure. This shows that the magnetic moment reorientates to the in-plane, and the average value of θ is about 76.2° under a pressure of 36 kbar. The final angle between the average magnetic moment direction and the film plane is only about 13.8° at a pressure of 36 kbar, which is very close to the film plane. This is in good agreement with the previous result for amorphous alloys [21], where for high pressure the spin direction is tilted more in the ribbon plane.

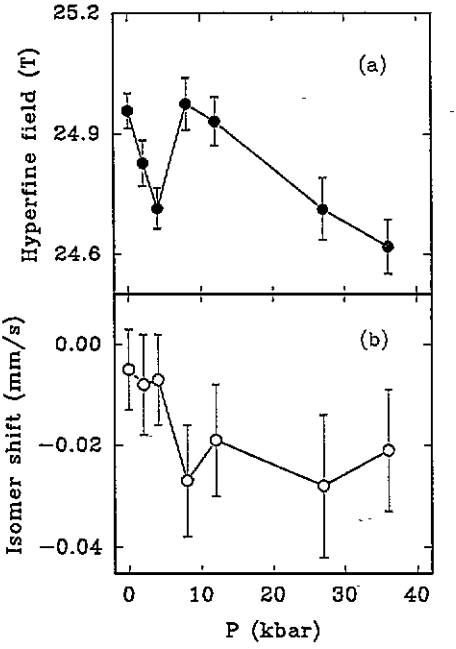

Figure 8. Pressure dependence of the hyperfine field (*a*) and the isomer shift (*b*) of the BCC 304 SS film.

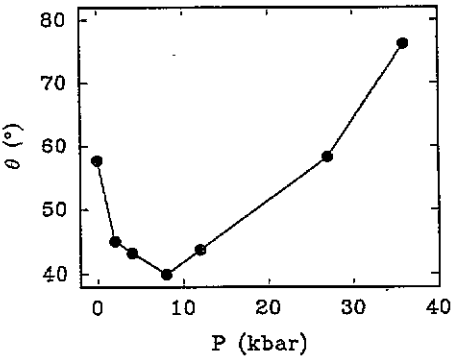

Figure 9. Pressure dependence of the angle θ between the γ-ray direction and the average magnetic moment direction of the BCC 304 SS film.

For weak magnetostriction anisotropy materials, when $\lambda_{100} = \lambda_{111} = \lambda_s$, the energy of the external stress, F_σ, can be simply written as [22]

$$F_\sigma = -\tfrac{3}{2}\lambda_s \sigma \cos^2 \phi \tag{4}$$

where λ_s is the stature magnetostriction, σ is the tension, and ϕ is the angle between the tension direction and magnetization direction. From (4), it can be found that for a magnetic material with positive λ_s under pressure, the stress energy F_σ is a minimum when $\phi = \frac{1}{2}\pi$ or $\phi = \frac{3}{2}\pi$, i.e. the pressure will lead to the magnetization of the material rotating to a direction perpendicular to the pressure (in-plane). This is in agreement with our experiment when the pressure is more than 8 kbar. In fact, the magnetostriction λ_s of many Fe-based alloys is positive, such as Fe–Al (13%Al), Fe–Co–V (2%V, 49%Co), Fe–Si(3%Si) and permalloy [23]. It is reasonable to conclude that the 304 SS film is positive magnetostriction, so the experimental results can be explained well by the external stress energy.

After the pressure is released, the Mössbauer spectrum is the same as that for the as-sputtering BCC 304 SS. This indicates that pressures up to 36 kbar cause elastic deformation, which is reversible by removing the pressure. From this point, it can be seen that the pressure and annealing obviously have a different influence on the direction of the magnetization of the BCC 304 SS film. The former is reversible; the latter is irreversible.

4. Conclusion

The studied results show that the non-iron atoms (Cr, Ni and Mn) in the BCC 304 SS have a clear influence on the local magnetic properties, whose magnitudes are closely related to the number and distance of the nearest-neighbour atoms. Each non-iron nearest-neighbour atom decreases the hyperfine field by about 2.3 T and the isomer shift by 0.01 mm s^{-1}. Furthermore, each next-nearest-neighbour non-iron atom is estimated to reduce the hyperfine field by about 1.2 T. The metastable BCC 304 SS is stable at an annealing temperature lower than 500 °C or a pressure up to 36 kbar. The transformation from the BCC to FCC state begins near 500 °C and is completed near 800 °C. The annealing and pressure both cause rotation of the easy magnetization direction, which tends to the out-of-plane at the annealing and a pressure up to 8 kbar, while it starts to reorientate to the in-plane when the pressure is larger than 8 kbar. The latter behavior is related to positive magnetostriction.

Acknowledgments

One of the authors (FSL) gratefully acknowledges financial support of the Volkswagenwerk Stiftung and Deuscheforschungsgemeinschaft (DFG) of Germany. This work was partially supported by the National Natural Science Foundation and State Key Magnetism Laboratory of China.

References

[1] Moriya T 1983 *J. Magn. Magn. Mater.* **31–4** 10
[2] Barbee T W, Jacobson B E and Keith D L 1979 *Thin Solid Films* **63** 143
[3] Childress J, Liu S H and Chien C L 1988 *J. Appl. Phys.* **64** 6059
[4] Childress J, Liu S H and Chien C L 1988 *J. Physique Coll.* C8 113

[5] Abd-Elmeguid M M, Micklitz H and Kaindl G 1981 *Phys. Rev.* B **23** 75
[6] Möller H S 1968 *Z. Phys.* **212** 107
[7] Czjzek G and Berger W G 1970 *Phys. Rev.* B **1** 957
[8] Hesse J and Rübartsch A 1974 *J. Phys. E: Sci. Instrum.* 7 526
[9] Dubiel S M and Zukrowski J 1981 *J. Magn. Magn. Mater.* **23** 214
[10] Dubiel S M and Zinn W 1983 *J. Magn. Magn. Mater.* **37** 237
[11] Dubiel S M and Zinn W 1982 *Phys. Rev.* B **26** 1574
[12] Dubiel S M and Zinn W 1982 *J. Magn. Magn. Mater.* **28** 261
[13] Miedema A R and van der Woude F 1980 *Physica* B **100** 145
[14] van der Kraan A M and Buschow K H J 1983 *Phys. Rev.* B **27** 2693
[15] Walker L R, Wertheim G K and Jaccarino V 1961 *Phys. Rev. Lett.* **6** 98
[16] Chien C L and Hasegawa R 1977 *Phys. Rev.* B **16** 3024
[17] Pipkorn D, Edge C K, Debrunner P, De Pasquali G, Drickamer H G and Frauenfelder H 1964 *Phys. Rev.* **135** A1604
[18] Williamson D L, Bukshpan S and Ingalls R 1972 *Phys. Rev.* B **6** 4194
[19] Johnson P C, Stein B A and Davis R S 1962 *J. Appl. Phys.* **33** 557
[20] Hoffman D W and Thornton J A 1977 *Thin Solid Films* **40** 355
[21] Abd-Elmeguid M M, Micklitz H and Vincze I 1982 *Phys. Rev.* B **25** 1
[22] Vonsovskii S V 1974 *Magnetism* vol 2 (New York: Wiley) p 946
[23] Heck I C 1974 *Magnetic Materials and their Applications* (Oxford: Butterworth) p 663